Hindawi
Mathematical Problems in Engineering
Volume 2018, Article ID 1897394, 11 pages
https://doi.org/10.1155/2018/1897394

Research Article

Simple Method to Predict Ground Displacements Caused by Installing Horizontal Jet-Grouting Columns

Zhi-Feng Wang[1], **Jack S. Shen**[2] **and Wen-Chieh Cheng**[3]

[1]*School of Highway, Chang'an University, Xi'an 710064, China*
[2]*Department of Civil and Construction Engineering, Swinburne University of Technology, Hawthorn, VIC 3122, Australia*
[3]*Institute of Tunnel and Underground Structure Engineering, Xi'an University of Architecture and Technology, Xi'an 710055, China*

Correspondence should be addressed to Zhi-Feng Wang; zhifeng.wang@chd.edu.cn

Received 4 May 2017; Accepted 26 December 2017; Published 30 January 2018

Academic Editor: Damijan Markovic

During the horizontal jet grouting in soft ground, injection of large volumes of water and grout into the soil can lead to significant ground displacements. A simple method is proposed in this paper to predict the ground displacements caused by installing horizontal jet-grouting columns. The process of installing a horizontal column is simplified as the expansion of a cylindrical cavity with a uniform radial stress applied at plastic-elastic interface in a half plane. In this study, the analytical solution is adopted to calculate the deformation induced by the expansion of a cylindrical cavity. Considering the main jetting parameters (jetting pressure of the fluid, flow rate of the fluid, and withdrawal rate of the rod) and the soil properties (stiffness of the surrounding soil), an empirical equation to estimate the radius of plastic zone is developed. Two field tests are carried out in Shanghai, China, to verify the correctness and applicability of the proposed method. Comparisons between the predicted and measured values indicate that the proposed method can provide a reasonable prediction. The proposed simple method can be recommended as a useful tool for the design of ground improvement by means of horizontal jet grouting.

1. Introduction

Jet grouting has been deemed as one of the most widely used ground improvement techniques for strengthening soft soil deposits and preventing groundwater seepage from leaking fractures or fissures [1–15]. Jet grouting is frequently used for the launching of shield machines or tunnel construction in complex geological conditions. Jet grouting technology is based on the injection of high velocity fluids through small-diameter nozzles to erode the soil and mix it with injected grout to form a soil-cement column [16–21]. Based on the different methods of fluid injection, jet-grouting technology can be classified as (a) single fluid system (grout only), (b) double fluid system (grout + air), or (c) triple fluid system (water + grout + air) [22–25]. Generally, according to the injection direction of the fluid, the jet-grouting technology can be divided into (i) vertical jet-grouting technology and (ii) horizontal jet-grouting technology.

Since there is a risk of intrusion of an overlying layer, horizontal jet-grouting technology has been increasingly used to create jet-grouting umbrellas for protecting excavations and reducing surface settlements (Xu et al., 2016) [4, 26–31]. As jet grouting involves the injection of large volumes of water or grout into the soil, inevitable disturbance of the surrounding soil will occur, which may cause significant displacement of the ground [4, 19, 32–37]. When jet-grouting columns are installed horizontally, the impact on the surrounding soil is mainly due to the vertical orientation of the jet, which is of great concern for geotechnical engineers. The ground displacement induced by the jet-grouting process may result in additional earth pressures being imposed on existing building foundations or utilities, causing possible adverse effects. Thus, it is necessary to determine the magnitude of such additional loads and the anticipated subsoil movement and ground surface heave.

Recent advances in jet-grouting technology have mainly focused on the strength of hardened columns and the evaluation of achievable column size (Wang et al., 2012) [38–41]. There is, however, very little literature discussing the ground displacement induced by horizontal jet-grouting

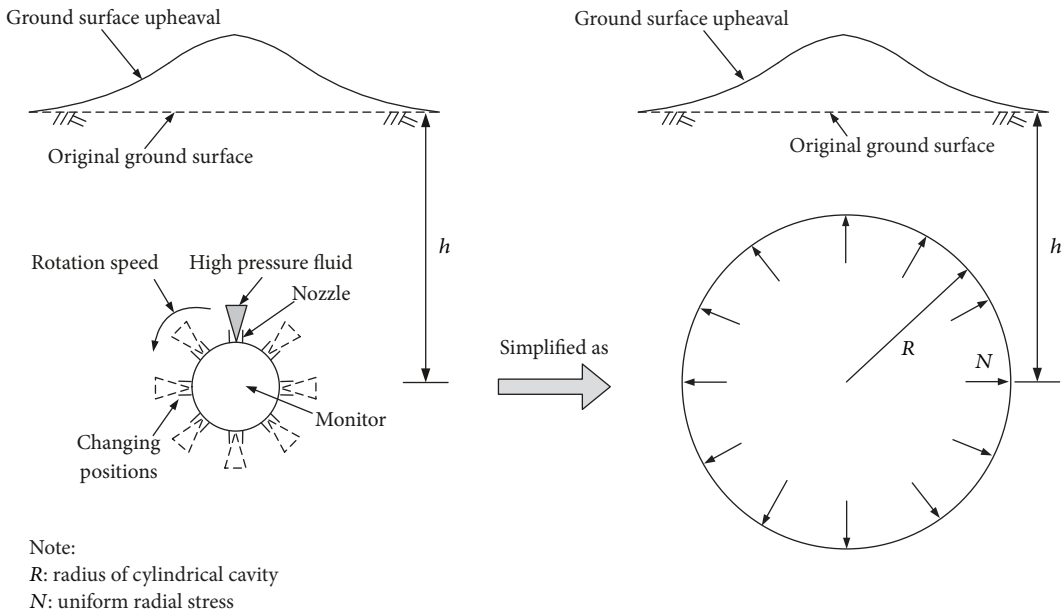

Note:
R: radius of cylindrical cavity
N: uniform radial stress

(a) Sectional view of the process of installing a horizontal column

(b) Expansion of a cylindrical cavity with uniform radial stress in a half plane

Figure 1: Schematic illustration of ground surface heave due to the construction of horizontal jet grouting.

column installation. Based on the cavity expansion theory, Chai et al. [42–44] proposed a semitheoretical method to estimate the lateral displacements induced by installing soil-cement columns. However, Chai's method was developed for the installation of vertical soil-cement columns and cannot be directly applied to the installation of horizontal jet-grouting columns.

In this paper, a method was proposed to predict the ground displacement caused by installing a horizontal jet-grouting column by considering the jetting parameters and soil properties. This was done by simplifying the process of installing a horizontal column as the expansion of a cylindrical cavity and with uniform radial stress in a half plane. The ground displacements from two field tests conducted in Shanghai, China, were compared with the predicted values to verify the correctness and applicability of the proposed method.

2. Brief Review of Existing Methods

There are three available methods for estimating ground displacement due to horizontal jet-grouting column installation: (i) the empirical method, (ii) the numerical simulation method, and (iii) the semitheoretical and semiempirical method.

Empirical methods are based upon field observations. However, the parameters used in the empirical methods due to a lack of the physical meaning were not defined clearly. Additionally, the parameters are usually derived for specific ground conditions and they are difficult to be applied to other jet-grouting projects that possess different ground conditions.

Numerical simulation methods are not convenient for practical use because of the requirement of the input parameters. Determining the input parameters involves professional background knowledge and the calibration of the input parameters by performing laboratory experiments may be required. Additionally, the numerical simulation methods may not be capable of modelling the process of jet-grouting column installation.

Semitheoretical and semiempirical methods are based upon the cavity expansion theory in an infinite soil mass. The methods may be capable of describing the process of jet-grouting column installation. The semitheoretical approach to estimate the lateral displacement caused by the installation of soil-cement columns was proposed by Chai et al. [42–44], in which the radius of the cavity (R_u), a key parameter, was empirically determined by analyzing several field tests using the slurry double mixing (SDM) method, the dry jet mixing (DJM) method, and the wet jet mixing (WJM) method. Notwithstanding that, this method can only be applied to the prediction of lateral displacement caused by vertical jet-grouting column installation. Also, the effect of the jetting pressure which plays a leading role for horizontal jet grouting cannot be considered in this method.

3. General Consideration for Simplification of Horizontal Jet-Grouting Process

During the installation of a horizontal jet-grouting column at a depth (h), the high pressure fluid is injected through small-diameter nozzles installed on the monitor, which is continuously rotated at a constant rate and slowly withdrawn, as shown in Figure 1(a). Since the jet-grouting process

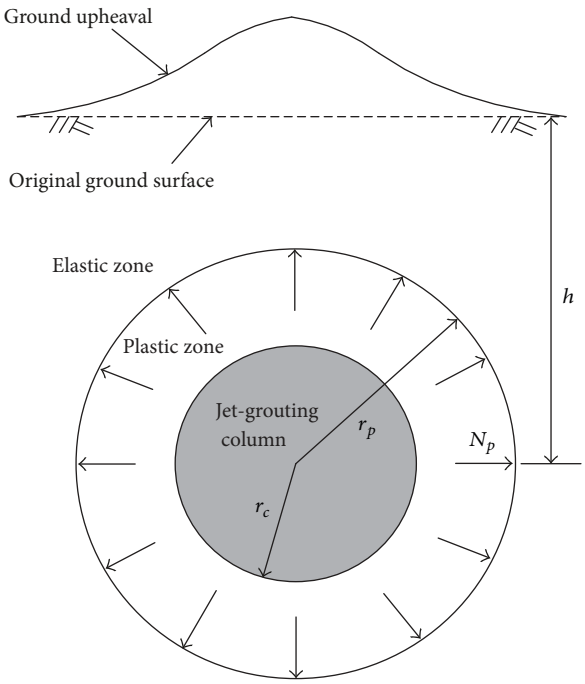

Note:
r_c: radius of jet-grouting column
r_p: radius of the plastic zone
N_p: stress at the interface of the plastic and the elastic zones

FIGURE 2: Stress state variation caused by the installation of horizontal jet grouting.

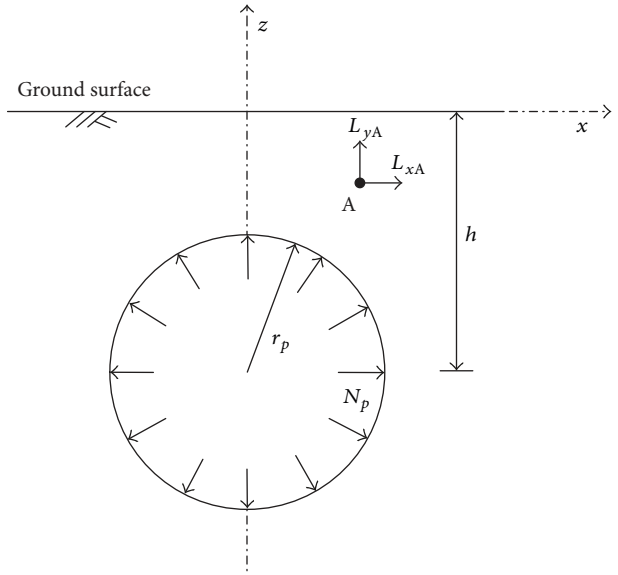

FIGURE 3: Parameters required for calculating the deformation with a uniform stress applied to the cylinder cavity boundary.

involves the injection of large volumes of water or grout into the soil, significant ground heave is expected. In this study, for simplicity purposes, it was assumed that the ground displacement due to the installation of a horizontal column was identical to the ground deformation induced by the expansion of a cylindrical cavity (R) with uniform radial stress (N) in a half plane, as shown in Figure 1(b). Due to the simplification, the following two questions are raised and discussed. (1) How can one calculate the ground deformation induced by the expansion of a cylindrical cavity with uniform radial stress in a half plane? (2) How can one describe the physical meaning of R and N and then determine their values?

Verruijt [45] developed an analytical solution for calculation of the deformation caused by the expansion of a cylindrical cavity with uniform radial stress in a half plane. In this paper, Verruijt's solution was utilized to calculate the ground displacements induced by the installation of a horizontal jet-grouting column. Figure 2 depicts the change in the stress state due to the installation of a horizontal jet-grouting column, and the influencing area can be divided into three parts: (i) jet-grouting column, (ii) plastic zone, and (iii) elastic zone. In this study, the two theoretical parameters, that is, the radius of a cylindrical cavity (R) and the uniform radial stress (N), were described as the plastic zone (r_p) and the stress at the interface of the plastic and elastic zones (N_p), respectively.

4. Ground Displacements Caused by Installation of a Single Column

4.1. Brief Review of Verruijt's Solution. Using the complex variable method, Verruijt [45] proposed equations for calculating the deformations caused by a uniform stress acted on the cavity boundary in a half plane. Considering the plastic zone (r_p) and the stress at the interface of the plastic and elastic zones (N_p), Figure 3 illustrates the parameters required for calculating the deformations, while the relevant equations are listed as follows:

$$L_{xA} = \mathrm{Re}\left(\frac{1+\upsilon}{E}\left((3-4\upsilon)\,f(Z) - Z\overline{f'(Z)} - \overline{F(Z)}\right)\right) \quad (1)$$

$$L_{yA} = \mathrm{Im}\left(\frac{1+\upsilon}{E}\left((3-4\upsilon)\,f(Z) - Z\overline{f'(Z)} - \overline{F(Z)}\right)\right), \quad (2)$$

where Re and Im represent the real and imaginary parameters respectively; L_{xA} is the displacement of point A in x direction; L_{yA} is the displacement of point A in y direction; υ is Poisson's ratio; E is Young's modulus; $Z = x + iy$; $f(Z)$ and $F(Z)$ are the analytic functions. Based on the solution of Verruijt [45], the equations to determine functions $f(Z)$, $F(Z)$, and $f'(Z)$ are derived as follows:

$$f(Z) = C_d\left(-2i\left(1+\eta^2\right) + 2i\frac{Z\left(1+\eta^2\right) + ih\left(1-\eta^2\right)}{Z\left(1+\eta^2\right) - ih\left(1-\eta^2\right)}\right.$$

$$+ 2i\eta^2 \frac{Z\left(1+\eta^2\right) - ih\left(1-\eta^2\right)}{Z\left(1+\eta^2\right) + ih\left(1-\eta^2\right)}\Bigg)$$

$$F(Z) = C_d\Bigg(-3i\left(1+\eta^2\right) + 2i\eta^2 \frac{Z\left(1+\eta^2\right) + ih\left(1-\eta^2\right)}{Z\left(1+\eta^2\right) - ih\left(1-\eta^2\right)} + i\left(\frac{Z\left(1+\eta^2\right) + ih\left(1-\eta^2\right)}{Z\left(1+\eta^2\right) - ih\left(1-\eta^2\right)}\right)^2 + 2i\frac{Z\left(1+\eta^2\right) - ih\left(1-\eta^2\right)}{Z\left(1+\eta^2\right) + ih\left(1-\eta^2\right)} + i\eta^2\left(\frac{Z\left(1+\eta^2\right) - ih\left(1-\eta^2\right)}{Z\left(1+\eta^2\right) + ih\left(1-\eta^2\right)}\right)^2\Bigg)$$

$$f'(Z) = C_d\left(\frac{4h\left(1-\eta^2\right)\left(1+\eta^2\right)}{\left(Z\left(1+\eta^2\right) - ih\left(1-\eta^2\right)\right)^2} - \frac{4\eta^2 h\left(1-\eta^2\right)\left(1+\eta^2\right)}{\left(Z\left(1+\eta^2\right) + ih\left(1-\eta^2\right)\right)^2}\right)$$

$$C_d = -\frac{\eta^2 N_p h}{\left(1-\eta^2\right)\left(1-\eta^4\right)}$$

$$\eta = \frac{h - \sqrt{h^2 - r_p^2}}{r_p}, \tag{3}$$

where h is the depth for installation of a horizontal column; N_p is the stress at the interface of the plastic and elastic zones; r_p is the radius of the plastic zone. In this study, calculations of the radius of plastic zone and the interface stress of the plastic and elastic zones based on the above equations have been implemented in the MATLAB environment.

4.2. Radius of Plastic Zone. There are two key factors that significantly affect the radius of the plastic zone (r_p), that is, soil properties and jetting parameters. As the soil properties are basically the same, the radius of the plastic zone (r_p) will be larger if the higher values of the jetting parameters are introduced. Contrarily, in the event that the jetting parameters are basically the same, the radius of the plastic zone (r_p) will be smaller if the values of the soil properties are higher. In this study, two parameters, E_n and E, were chosen to represent the influence of the jetting parameters and soil properties on the r_p value, as depicted in Figure 4, and their relationship can be expressed by the following equation:

$$r_p = f\left(E_n, E\right), \tag{4}$$

where E_n is the injected energy for the unit length of jet-grouting column; E is Young's modulus. Thus, the following

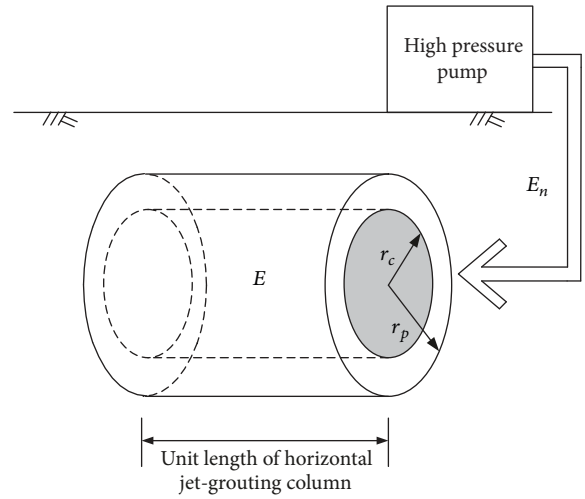

Figure 4: Parameters required for calculating the radius of the plastic zone (R_p) for horizontal jet grouting.

empirical equation to determine the parameter r_p was proposed for implementing the dimensional analysis:

$$r_p = \alpha_p \sqrt{\frac{E_n}{E}}, \tag{5}$$

where α_p is a parameter that is related to the soil types.

E_n is related to the treatment energy for the unit length of jet-grouting column at the pump (E_p). Generally, the following equation is adopted to calculate the E_n value:

$$E_n = \beta E_p = \beta \frac{pQ}{v_s}, \tag{6}$$

where E_p is the treatment energy for the unit length of jet-grouting column at the pump; β is reduction coefficient that considers the energy losses in the transportation of jetting fluid to the nozzle; p is the injection pressure at the pump; Q is the flow rate; v_s is the average withdrawal speed of the monitor. β value of 0.8 suggested by Croce and Flora [22] has been adopted in this study.

4.3. Stress at the Plastic-Elastic Zone Interface (N_p). The factors that primarily affect the stress at the plastic-elastic zone interface (N_p) are related to the shear strength and stress state of ground soil. Vesic [46] proposed the following equations to determine the stress at the plastic-elastic zone interface (N_p):

$$N_p = \left(c \cdot F_c + p_0 \cdot F_q + c \cdot \cot\varphi\right) \cdot \left(\sqrt{I_{rr}\sec\varphi}\right)^{2\sin\varphi/(1+\sin\varphi)} - c \cdot \cot\varphi \tag{7}$$

$$F_q = \left(1+\sin\varphi\right)\left(\frac{I_r}{1 + I_r \cdot \Delta \cdot \sec\varphi}\sec\varphi\right)^{\sin\varphi/(1+\sin\varphi)} \tag{8}$$

$$F_c = \left(F_q - 1\right)\cot\varphi \tag{9}$$

$$I_{rr} = \frac{I_r}{1 + I_r \cdot \Delta \cdot \sec\varphi} \tag{10}$$

$$I_r = \frac{E}{2(1+\upsilon)(c + p_0 \cdot \tan\varphi)}, \tag{11}$$

where c is cohesion of soil; F_c and F_q are coefficients for cylindrical cavity; φ is internal friction angle; E is Young's modulus; Δ is average volumetric strain; υ is Poisson's ratio; I_r is rigidity index; I_{rr} is reduced rigidity index; p_0 is initial mean normal stress, which can be calculated as $p_0 = ((2+K_0)/3)\sigma_{v0}$ in the case of horizontal jet grouting. For the case of $\varphi = 0$ and zero volumetric strain ($\Delta = 0$), the following simple equation to calculate σ_p can be obtained:

$$N_p = c_u + \frac{2 + K_0}{3}\sigma_{v0}, \tag{12}$$

where c_u is the undrained shear strength of the soil; K_0 is the at-rest horizontal earth pressure coefficient; σ_{v0} is the initial vertical stress.

4.4. Calculation Procedure for Ground Displacements in Elastic Zone. Figure 5 points out the parameters required for calculating the ground movement in the elastic zone ($R_A \geq r_p$). The procedure for calculating the ground displacements in the elastic zone is summarized as follows.

(1) Calculating the Stress at the Plastic-Elastic Zone Interface (N_p). Soil properties (unit weight, undrained shear strength, and at-rest earth pressure coefficient) can be first derived from ground investigations and/or laboratory experiments. For a given depth of construction, the stress at the plastic-elastic zone interface (N_p) can be calculated using (12).

(2) Calculating the Radius of the Plastic Zone (r_p). The jetting parameters (i.e., injection pressure at pump, flow rate, and average withdrawal speed of monitor) are collected, and Young's modulus of soil is tested. Then the radius of the plastic zone (r_p) can be calculated using (5) and (6).

(3) Calculating the Ground Displacements in the Elastic Zone. By the calculated values of N_p and r_p, the ground displacements in the elastic zone can thus be calculated using (1) and (2).

4.5. Calculation Procedure for Ground Displacements in Plastic Zone. Figure 6 points out the parameters required for calculating the ground movement in the plastic zone ($r_c \leqq R_A \leqq r_p$). Since Verruijt [45] solution cannot be utilized for calculating the ground displacements in a straightforward manner, by referring to an approximate formula from Chai et al. [42], two equations to calculate the ground displacements in plastic zone are proposed:

$$L_{xA} \approx L_p \frac{2r_p + L_p}{2R_A + L_p r_p / R_A} \frac{x}{R_A} \tag{13}$$

$$L_{yA} \approx L_p \frac{2r_p + L_p}{2R_A + L_p r_p / R_A} \frac{h + y}{R_A}, \tag{14}$$

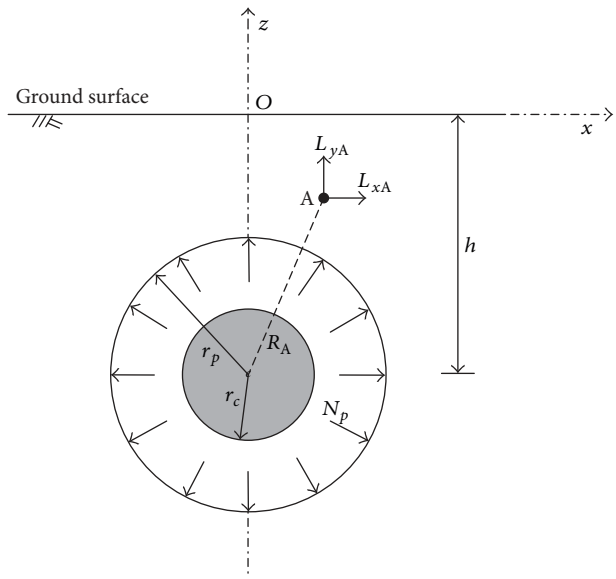

Figure 5: Parameters required for calculating the ground movement in the elastic zone ($R_A \geq r_p$).

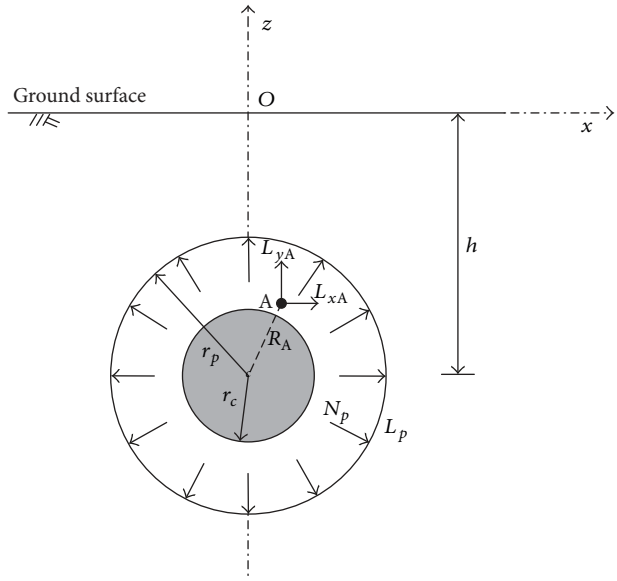

Figure 6: Parameters required for calculating the ground movement in the plastic zone ($r_c \leq R_A \leq r_p$).

where L_p is the soil displacement at the radius of plastic zone; R_A is the distance from the column center to point A, which can be calculated by $R_A = \sqrt{x^2 + (h+y)^2}$. The calculation procedure for the ground displacements in plastic zone is described as follows.

(1) Calculating the Soil Displacement at the Radius of Plastic Zone (L_p). The radius of the plastic zone (r_p) and the stress at the plastic-elastic zone interface (N_p) can be calculated through the obtained soil parameters and jetting parameters. After that, the soil displacement at the radius of plastic zone

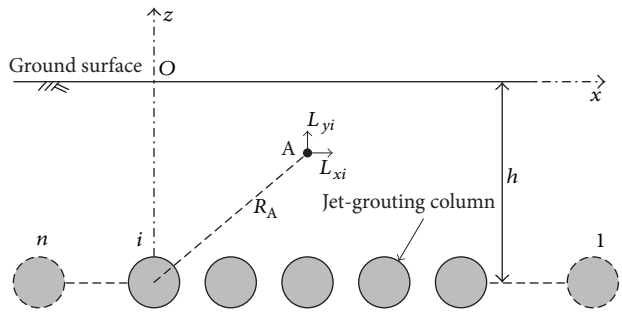

Figure 7: Schematic illustration of the ground displacements caused by the installation of a row of columns.

(L_p) can be calculated using the calculated values of N_p and r_p and (1)and (2).

(2) Calculating the Ground Movement in the Plastic Zone. The ground movement in the plastic zone can be calculated by substituting the calculated values of L_p and r_p into (13) and (14).

5. Ground Displacements Induced by Installation of a Row of Columns

As a series of rows of horizontal jet-grouting columns are installed at a worksite, the ground displacements are likely to be influenced by the installation sequence and rheological properties of the grout. It was assumed that superposition principle can be applied to calculate the ground displacements induced by the installation of horizontal jet-grouting columns. Thus, the ground movement at point A induced by the installation of a row of columns will be equal to the summation of the effect resulting from each individual column installation, as shown in Figure 7 and the following equation:

$$L_{xA} = \sum_{i=1}^{n} L_{xi}$$
$$L_{yA} = \sum_{i=1}^{n} L_{yi}, \quad (15)$$

where i represents the number of the jet-grouting columns; L_{xi} is the displacement of point A in x direction due to the installation of the jet-grouting column numbered i; L_{yi} is the displacement of point A in y direction due to the installation of the column numbered i.

The procedure of utilizing the proposed simple method for predicting the ground displacements induced by installing horizontal jet-grouting columns is described as follows.

(1) Based upon the energy imposed during jetting and Young's modulus of soil, the radius of the plastic zone (r_p) can be calculated using (5).

(2) The stress at the plastic-elastic zone interface (N_p) can then be calculated by substituting the undrained shear strength of soil, c_u, and the coefficient of lateral earth pressure at rest, k_0, into (12).

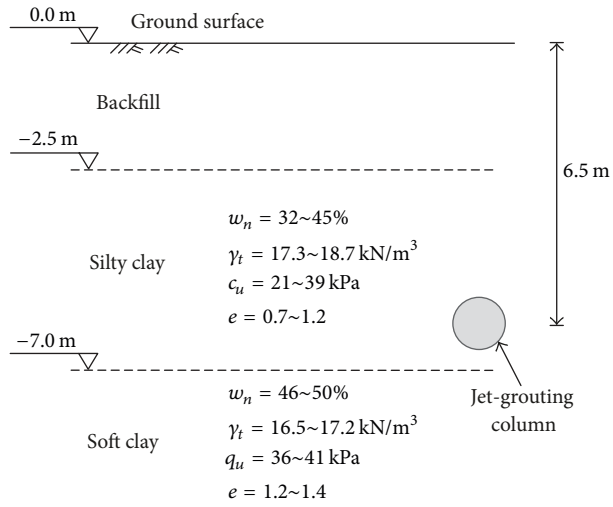

Figure 8: Geotechnical profile and soil properties (single column installation case): γ_t, unit weight; w_n, water content; e, void ratio; q_u, unconfined compressive strength.

(3) The associated ground displacements in the elastic zone and in the plastic zone induced by installing a horizontal jet-grouting column can be calculated using (1) and (2) and (13)-(14), respectively.

(4) The ground displacements caused by installing a row of horizontal jet-grouting columns would be identical to the summation of the effects of each jet-grouting column installation and can be calculated using (15).

It should be noted that the method in the previous publication of the authors [19] is developed for analyzing the vertical jet grouting cases, but the authors found that Shen et al.'s method cannot be directly used to obtain a reasonable displacement prediction for the horizontal jet grouting cases in engineering practice. Thus, a new approach is developed in this paper to provide a reasonable displacement prediction for horizontal jet grouting cases. Additionally, two case histories (horizontal jet grouting cases), which are entirely different from the case histories (vertical jet-grouting cases) in Shen et al. [19], are analyzed to verify the applicability of the newly developed approach. An improved equation to calculate the parameter r_p is also provided considering E_n and E in this paper (see (5)), which is also different from the equation in Shen et al. [19] (see 9). Moreover, because the boundary conditions for vertical and horizontal jet-grouting cases are different, the equation to calculate the value of N_p (see (12)) in this new manuscript is also different from the equation in Shen et al.'s [19] paper (see 16).

6. Method Verification

6.1. Single Column Installation. Shen et al. [4] reported on a field test located near the Huangpu River in the Pudong New Development Area, China. In this field test, the single fluid system was used for horizontal jet grouting, where the metro tunnel stating shaft was protected by the excavation (Wu et al., 2015c; 2016; 2017a, b) [19, 47, 48]. Figure 8 shows the geotechnical profile and soil properties for this case history.

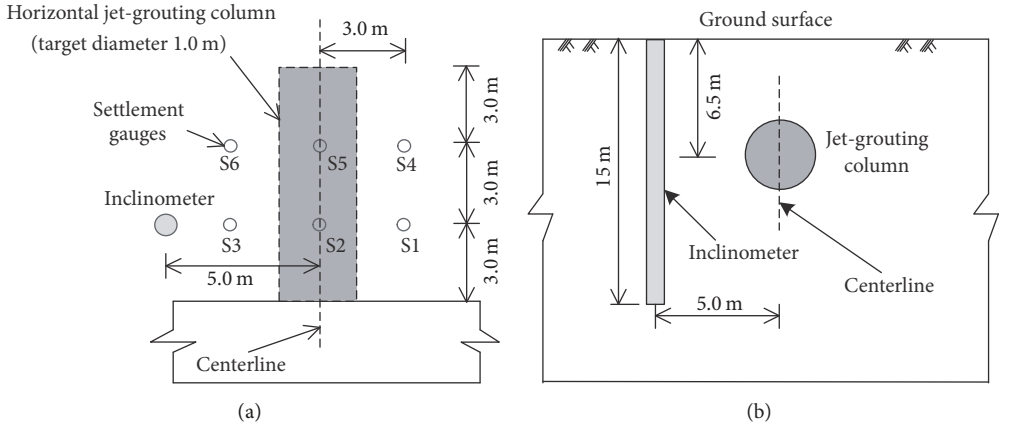

Figure 9: Plan and sectional view of the layout of ground settlement gauges and inclinometer (single column installation case).

The subsoil profile consists mainly of three soil layers: backfill, silty clay, and soft clay. The water content for the soils on this test site ranged from 32% to 45%, while the undrained shear strengths were in the range of 21–39 kPa.

The ground surface heave and lateral displacement during the installation of a horizontal jet-grouting column were monitored. Six ground settlement gauges (S1 to S6) spaced at 3.0 m were installed, and one soil inclinometer was set at a depth of 15 m, as shown in Figures 9(a) and 9(b). The horizontal jet-grouting column was installed at a depth of 6.5 m. Jetting parameters for this field test were as follows: the jetting pressure (p) = 30 MPa; the flow rate (Q) = 90 L/min; and the withdrawal rate of the rod (v_s) = 15 cm/min. By (6), the E_n value was calculated to be 14.4 MJ/m. Then, by c_u = 30 kPa and K_0 = 0.5, the N_p value was calculated to be 127 kPa. For silty clay, the constrained modulus (E) of about 5.0 MPa reported by Huang and Gao [49], Shen and Xu [50], Tan and Wei [51], Ye et al. (2013), Du et al. [52], and Shen et al. [53] was used in the calculation. As discussed previously, the empirical parameter (α_p) related to the soil types is an unknown parameter and is difficult to determine. It is noted from a trial calculation that the predicted lateral displacements caused by the installation of a single column were in good agreement with the measured lateral displacements, with the α_p value set to 1.0.

Substituting the calculated values of E_n, E, and α_p into (5), the r_p value was calculated to be 1.70 m. Substituting the values of r_p, N_p, and h into (1) to (3), which were coded in MATLAB, the ground surface heave and the lateral displacement caused by the installation of a horizontal column can be obtained. Figure 10 presents comparisons for the predicted and measured values of the ground surface heave, caused by the installation of a horizontal column. As evident, the proposed method can provide a reasonable prediction. Additionally, the comparisons of the predicted and measured values of the lateral displacement appear to be quite satisfactory (Figure 11).

6.2. Group Column Installation. Wang et al. [32] reported on a case history related to a field trial involving the installation of five horizontal jet-grouting columns at the entrance shaft

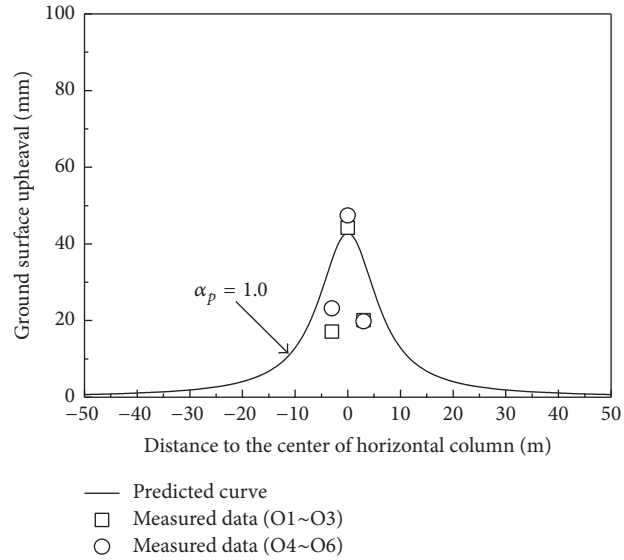

Figure 10: Comparisons of predicted and measured values of ground surface heave caused by installation of a horizontal column.

of Bailixincun Road Station of Shanghai Metro line 11. The jet-grouting columns in this field trial were formed using the double fluid method, known as the horizontal twin-jet-grouting method. Figure 12 shows the geotechnical profile and soil properties for this case history. The subsoil profile consisted of backfill (from 0.0 to 1.6 m), clayey silt (from 1.6 to 3.7 m deep), soft silty clay (from 3.7 to 13.0 m deep), and soft clay (from 13.0 to 27.0 m deep). Typical soil properties are summarized in Figure 12. The jet-grouting field test was conducted in the soft silty clay layer of low shear strength, which is subjected to time-dependent compressibility due to creep behavior (Wu et al. 2015d, e; Wu et al. 2017a, b) [54–56]. The soft soils were normal to slightly overconsolidated and were classified as low plasticity clays (CL), based on the Unified Soil Classification System (USCS). The water content of these soils varies from 30% to 50%, with unconfined compressive strengths (q_u) varying between 30 and 55 kPa.

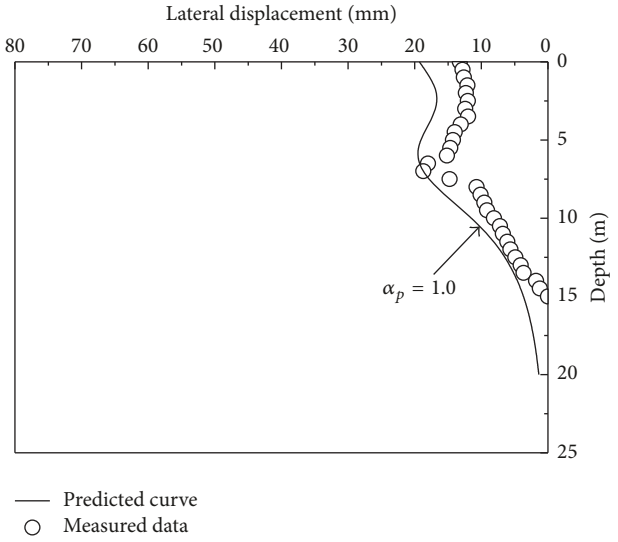

Figure 11: Comparison of the predicted and measured values of the lateral displacement caused by the installation of a horizontal column.

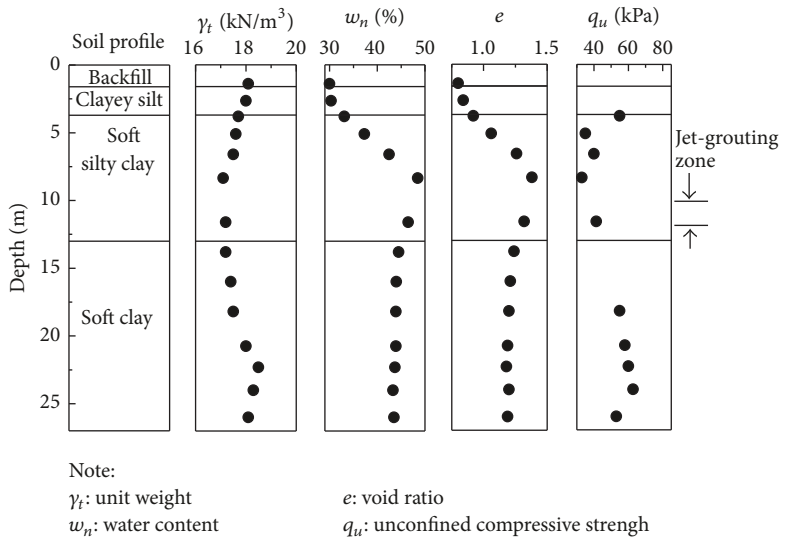

Figure 12: Geotechnical profile and soil properties (group column installation case).

In this field trial, due to the installation of five horizontal jet-grouting columns, the lateral displacement of subsoil and the ground surface heave were monitored. Figures 13 and 14 present the plan and sectional view of the layout of the ground settlement gauges and inclinometer for this case history. The instruments installed and monitored included one soil inclinometer and five ground settlement gauges (S1 to S5). The inclinometer was installed at a depth of 24 m, while the five horizontal columns were constructed at a depth range of 10.75–11.65 m. The construction sequence of the five horizontal columns was from C1 to C5, and their installations were completed in two days. In this case history, jetting parameters of the field test were as follows: the jetting pressure (p) = 12 MPa; the flow rate (Q) = 86 L/min; the withdrawal rate of the rod (v_s) = 60 cm/min. By (6), the E_n value was calculated to be 1.4 MJ/m. Substituting the c_u and K_0 values of 17.5 kPa and 0.5, respectively, into (7), the value of N_p was calculated to be 171 kPa. For soft silty clay, the constrained modulus (E) reported by Huang and Gao [49] and Tan and Li [57] is about 2.1 MPa. Substituting E_n = 1.4 MJ/m, E = 2.1 MPa, and α_p = 1.0 into (5), the value of r_p was 0.81 m.

Substituting the values of r_p, N_p, and h into the MATLAB program that was written to solve (1) to (3) and due to the installation of five horizontal columns, the ground surface heave and the lateral displacements can be calculated. Figures 15 and 16 plot comparisons between the predicted and measured values of the ground surface heave and the lateral displacement caused by the installation of five horizontal columns, respectively. As evident, there were some discrepancies between the predicted and measured values, likely due to the omission of the influence of installation sequence and rheological properties of the grout in the calculation. Moreover, after the construction of horizontal columns, either their very low initial strengths or the dissipation of

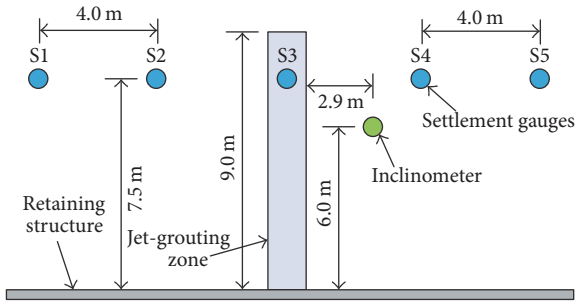

Figure 13: Plan view of the layout of ground settlement gauges and inclinometer (group column installation case).

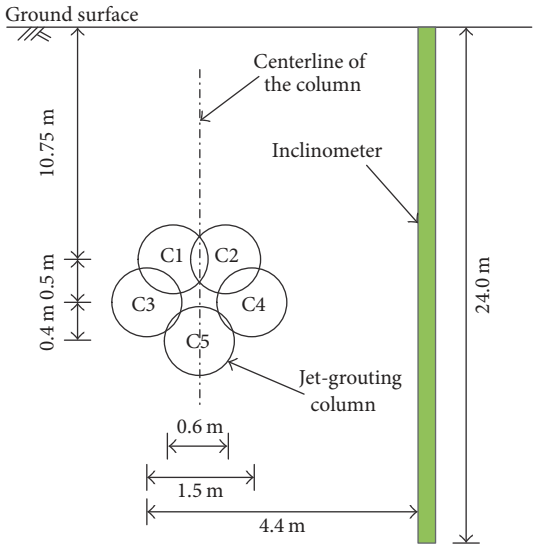

Figure 14: Sectional view of the layout of ground settlement gauges and inclinometer (group column installation case).

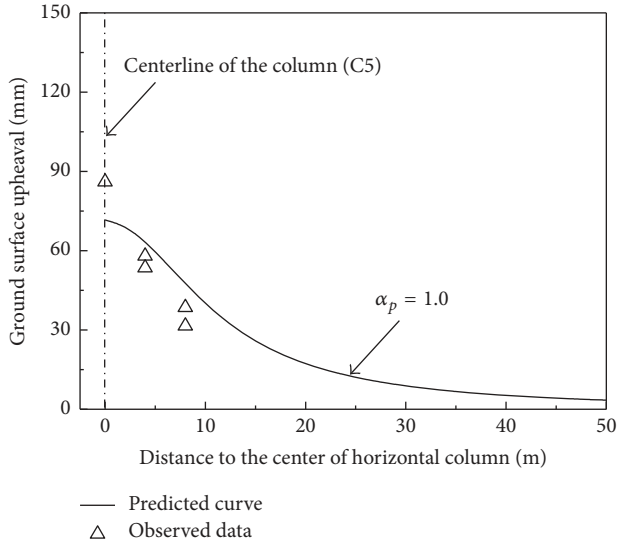

Figure 15: Comparisons of the predicted and measured values of the ground surface heave caused by the installation of five horizontal columns.

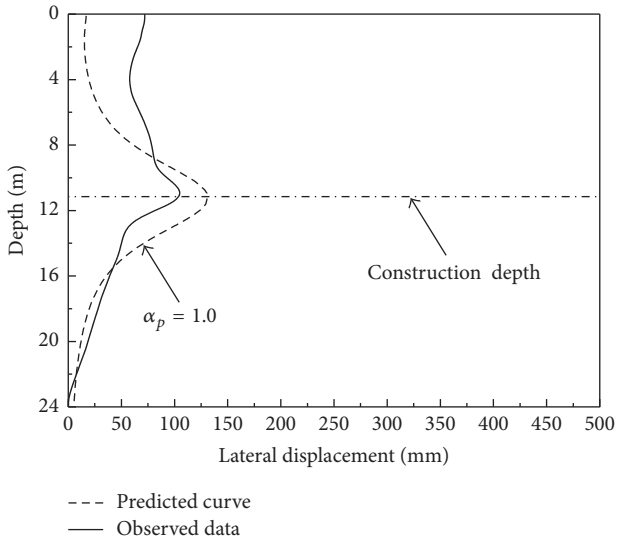

Figure 16: Comparisons of the predicted and measured values of the lateral displacement caused by the installation of five horizontal columns.

excess pore water pressure generated during construction could result in a reduction in the ground surface heave.

7. Conclusions

In this paper, a simple method to predict the ground displacements induced by installing horizontal jet-grouting columns was proposed. In this method, Verruijt [45] solution for calculating deformations based on the expansion theory of a cylindrical cavity with uniform radial stress in a half plane was adopted. An empirical equation to consider the total applied energy and soil properties to estimate the radius of plastic zone was developed. Based upon the comparisons between the measured ground displacements and those predicted through the proposed method, the following conclusions can be drawn:

(1) The proposed method was applied to two case histories to verify its correctness and applicability, in which one involved the installation of a horizontal column and the other involved the installation of five horizontal columns.

(2) The comparisons between the predicted and measured values of the lateral displacement and the ground surface heave showed that, in the single column installation case, the proposed method can yield a satisfactory prediction as the α_p value was set to 1.0. In the group column installation case, there were several discrepancies between the predicted and measured values, which were most likely due to the omission of the influence of installation sequence and rheological properties of the grout in the calculation procedure.

(3) Despite the discrepancies, the proposed method is deemed appropriate in guiding and improving the design of ground improvement by horizontal jet grouting.

Conflicts of Interest

The authors declare that there are no conflicts of interest regarding the publication of this paper.

Acknowledgments

The research work described herein was funded by the National Natural Science Foundation of China (NSFC) (Grant no. 41702287), the Fundamental Research Funds for the Central Universities (Grant no. 310821161022), and China Postdoctoral Science Foundation (2015M570803 and 2016T90877). The financial support is gratefully acknowledged. The authors are also grateful to Professor Arul Arulrajah for his help with the improvement of English language in this paper.

References

[1] J. Han, S. Oztoprak, R. L. Parsons, and J. Huang, "Numerical analysis of foundation columns to support widening of embankments," *Computers & Geosciences*, vol. 34, no. 6, pp. 435–448, 2007.

[2] C. E. Ho, "Analysis of deep jet grouting field trial in clay," in *Proceedings of the International Foundation Congress and Equipment Expo*, pp. 233–240, Orlando, Fl, USA, 2009.

[3] S.-L. Shen, Z.-F. Wang, S. Horpibulsuk, and Y.-H. Kim, "Jet grouting with a newly developed technology: the twin-jet method," *Engineering Geology*, vol. 152, pp. 87–95, 2013.

[4] S.-L. Shen, Z.-F. Wang, W.-J. Sun, L.-B. Wang, and S. Horpibulsuk, "A field trial of horizontal jet grouting using the composite-pipe method in the soft deposits of Shanghai," *Tunnelling and Underground Space Technology*, vol. 35, pp. 142–151, 2013.

[5] J. C. Ni and W.-C. Cheng, "Shield machine disassembly in grouted soils outside the ventilation shaft: a case history in Taipei Rapid Transit System (TRTS)," *Tunnelling and Underground Space Technology*, vol. 26, no. 2, pp. 435–443, 2011.

[6] J. C. Ni, W.-C. Cheng, and L. Ge, "A case history of field pumping tests in a deep gravel formation in the Taipei Basin, Taiwan," *Engineering Geology*, vol. 117, no. 1-2, pp. 17–28, 2011.

[7] J. C. Ni and W.-C. Cheng, "Characterising the failure pattern of a station box of taipei rapid transit system (TRTS) and its rehabilitation," *Tunnelling and Underground Space Technology*, vol. 32, pp. 260–272, 2012.

[8] J. C. Ni, W.-C. Cheng, and L. Ge, "A simple data reduction method for pumping tests with tidal, partial penetration, and storage effects," *Soils and Foundations*, vol. 53, no. 6, pp. 894–902, 2013.

[9] J. C. Ni and W.-C. Cheng, "Quality control of double fluid jet grouting below groundwater table: case history," *Soils and Foundations*, vol. 54, no. 6, pp. 1039–1053, 2014.

[10] J. C. Ni and W.-C. Cheng, "Field response of high speed rail box tunnel during horizontal grouting," *Journal of Testing and Evaluation*, vol. 43, no. 2, pp. 398–413, 2015.

[11] X. Gao, Y. Wei, and W. Huang, "Critical aspects of scanning probe microscopy mapping when applied to cement pastes," *Advances in Cement Research*, pp. 1–25, 2017.

[12] C. E. Ho and S. Hu, "Design optimization of underground subway station diaphragm walls using numerical modeling," in *Proceedings of the 2014 Congress on Geo-Characterization and Modeling for Sustainability, Geo-Congress*, pp. 3122–3132, USA, February 2014.

[13] J. Lai, X. Wang, J. Qiu et al., "A state-of-the-art review of sustainable energy based freeze proof technology for cold-region tunnels in China," *Renewable & Sustainable Energy Reviews*, vol. 82, pp. 3554–3569, 2018.

[14] J. X. Lai, H. Zhou, K. Wang et al., "Shield-driven induced ground surface and Ming Dynasty city wall settlement of Xi'an metro," *Tunnelling and Underground Space Technology*, 2018.

[15] C. E. Ho, "Groundwater management for sustainable underground subway development in Manhattan, New York City," in *Proceedings of the 1st Geo-Chicago Conference: Sustainability and Resiliency in Geotechnical Engineering, Geo-Chicago*, pp. 663–672, USA, August 2016.

[16] G. Modoni, A. Flora, S. Lirer, M. Ochmański, and P. Croce, "Design of jet grouted excavation bottom plugs," *Journal of Geotechnical and Geoenvironmental Engineering*, vol. 142, no. 7, Article ID 04016018, 2016.

[17] Z.-F. Wang, S.-L. Shen, W.-C. Cheng, and Y.-S. Xu, "Ground fissures in Xi'an and measures to prevent damage to the Metro tunnel system due to geohazards," *Environmental Earth Sciences*, vol. 75, no. 6, article no. 511, 2016.

[18] S.-L. Shen, Y.-X. Wu, and A. Misra, "Calculation of head difference at two sides of a cut-off barrier during excavation dewatering," *Computers & Geosciences*, vol. 91, pp. 192–202, 2017.

[19] S. L. Shen, Z. F. Wang, and W. C. Cheng, "Estimation of lateral displacement induced by jet grouting in clayey soils," *Géotechnique*, vol. 67, no. 7, pp. 621–630, 2017.

[20] W.-C. Cheng, Q.-L. Cui, J. S.-L. Shen, A. Arulrajah, and D.-J. Yuan, "Fractal prediction of grouting volume for treating karst caverns along a shield tunneling alignment," *Applied Sciences*, vol. 7, no. 7, article no. 652, 2017.

[21] Y. Wei, X. Gao, F. Wang, and Y. Zhong, "Nonlinear strain distribution in a field-instrumented concrete pavement slab in response to environmental effects," *Road Materials and Pavement Design*, pp. 1–14, 2017.

[22] P. Croce and A. Flora, "Analysis of single-fluid jet grouting," *Géotechnique*, vol. 50, no. 6, pp. 739–748, 2000.

[23] T. Y. Poh and I. H. Wong, "A field trial of jet-grouting in marine clay," *Canadian Geotechnical Journal*, vol. 38, no. 2, pp. 338–348, 2001.

[24] G. K. Burke, "Jet grouting systems: advantages and disadvantages," in *Proceedings of the GeoSupport Conference*, pp. 875–886, Orlando, Fl, USA, 2004.

[25] Y. S. Fang, C. C. Kao, J. Chou, K. F. Chain, D. R. Wang, and C. T. Lin, "Jet grouting with the superjet-midi method," *Ground Improvement*, vol. 10, no. 2, pp. 69–76, 2006.

[26] S. Coulter and C. D. Martin, "Effect of jet-grouting on surface settlements above the Aeschertunnel, Switzerland," *Tunnelling and Underground Space Technology*, vol. 21, no. 5, pp. 542–553, 2006.

[27] S.-L. Shen, H.-N. Wu, Y.-J. Cui, and Z.-Y. Yin, "Long-term settlement behaviour of metro tunnels in the soft deposits of Shanghai," *Tunnelling and Underground Space Technology*, vol. 40, pp. 309–323, 2014.

[28] J. Lai, S. He, J. Qiu et al., "Characteristics of seismic disasters and aseismic measures of tunnels in Wenchuan earthquake," *Environmental Earth Sciences*, vol. 76, no. 2, article 94, 2017.

[29] S.-L. Shen, Q.-L. Cui, C.-E. Ho, and Y.-S. Xu, "Ground response to multiple parallel microtunneling operations in cemented silty clay and sand," *Journal of Geotechnical and Geoenvironmental Engineering*, vol. 142, no. 5, Article ID 04016001, 2016.

[30] J. Qiu, X. Wang, S. He, H. Liu, J. Lai, and L. Wang, "The catastrophic landside in Maoxian County, Sichuan, SW China, on June 24, 2017," *Natural Hazards*, vol. 89, no. 3, pp. 1485–1493, 2017.

[31] J. Qiu, Y. Xie, H. Fan, Z. Wang, and Y. Zhang, "Centrifuge modelling of twin-tunnelling induced ground movements in loess strata," *Arabian Journal of Geosciences*, vol. 10, no. 22, 2017.

[32] Z.-F. Wang, S.-L. Shen, C.-E. Ho, and Y.-H. Kim, "Investigation of field-installation effects of horizontal twin-jet grouting in Shanghai soft soil deposits," *Canadian Geotechnical Journal*, vol. 50, no. 3, pp. 288–297, 2013.

[33] Z.-F. Wang, X. Bian, and Y.-Q. Wang, "Numerical approach to predict ground displacement caused by installing a horizontal jet grout column," *Marine Georesources & Geotechnology*, vol. 35, no. 7, pp. 970–977, 2017.

[34] W. Cheng, J. C. Ni, and S. Shen, "Experimental and analytical modeling of shield segment under cyclic loading," *International Journal of Geomechanics*, vol. 17, no. 6, Article ID 04016146, 2017.

[35] W. Cheng, J. C. Ni, J. S. Shen, and H. Huang, "Investigation into factors affecting jacking force: a case study," *Proceedings of the Institution of Civil Engineers—Geotechnical Engineering*, vol. 170, no. 4, pp. 322–334, 2017.

[36] W.-C. Cheng, J. C. Ni, and Y.-H. Cheng, "Alternative shoring for mitigation of pier-foundation excavation disturbance to an existing freeway," *Journal of Performance of Constructed Facilities*, vol. 31, no. 5, Article ID 04017072, 2017.

[37] J. L. Qiu, H. Q. Liu, J. X. Lai, H. P. Lai, J. X. Chen, and K. Wang, "Investigating the long term settlement of a tunnel built over improved loessial foundation soil using jet grouting technique," *Journal of Performance of Constructed Facilities*, 2018.

[38] M. Shibazaki, "State of practice of jet grouting," in *Proceedings of the Third International Conference on Grouting and Ground Treatment*, pp. 198–217, New Orleans, La, USA, 2003.

[39] C. E. Ho, "Fluid-soil interaction model for jet grouting," in *Proceedings of the Geo-Denver*, pp. 1–10, Denver, Co, USA, 2007.

[40] A. Flora, G. Modoni, S. Lirer, and P. Croce, "The diameter of single, double and triple fluid jet grouting columns: prediction method and field trial results," *Géotechnique*, vol. 63, no. 11, pp. 934–945, 2013.

[41] S.-L. Shen, Z.-F. Wang, J. Yang, and C.-E. Ho, "Generalized approach for prediction of jet grout column diameter," *Journal of Geotechnical and Geoenvironmental Engineering*, vol. 139, no. 12, pp. 2060–2069, 2013.

[42] J.-C. Chai, N. Miura, and H. Koga, "Lateral displacement of ground caused by soil-cement column installation," *Journal of Geotechnical and Geoenvironmental Engineering*, vol. 131, no. 5, pp. 623–632, 2005.

[43] J.-C. Chai, N. Miura, and H. Koga, "Closure to "Lateral displacement of ground caused by soil-cement column installation" by Jin-Chun Chai,Norihiko Miura, and Hirofumi Koga," *Journal of Geotechnical and Geoenvironmental Engineering*, vol. 133, no. 1, pp. 124–126, 2007.

[44] J. Chai, J. P. Carter, N. Miura, and H. Zhu, "Improved prediction of lateral deformations due to installation of soil-cement columns," *Journal of Geotechnical and Geoenvironmental Engineering*, vol. 135, no. 12, Article ID 005912QGT, pp. 1836–1845, 2009.

[45] A. Verruijt, "Deformations of an elastic half plane with a circular cavity," *International Journal of Solids and Structures*, vol. 35, no. 21, pp. 2795–2804, 1998.

[46] A. S. Vesic, "Expansion of cavities in infinite soil mass," *Journal of Soil Mechanics and Foundation Engineering*, vol. 98, no. SM3, pp. 265–290, 1972.

[47] H.-N. Wu, S.-L. Shen, S.-M. Liao, and Z.-Y. Yin, "Longitudinal structural modelling of shield tunnels considering shearing dislocation between segmental rings," *Tunnelling and Underground Space Technology*, vol. 50, pp. 317–323, 2015.

[48] H.-N. Wu, S.-L. Shen, L. Ma, Z.-Y. Yin, and S. Horpibulsuk, "Evaluation of the strength increase of marine clay under staged embankment loading: a case study," *Marine Georesources & Geotechnology*, vol. 33, no. 6, pp. 532–541, 2015.

[49] S. M. Huang and D. Z. Gao, *Foundation and Underground Engineering in Soft Ground*, China Architecture and Building Press, Beijing, 2005.

[50] S.-L. Shen and Y.-S. Xu, "Numerical evaluation of land subsidence induced by groundwater pumping in Shanghai," *Canadian Geotechnical Journal*, vol. 48, no. 9, pp. 1378–1392, 2011.

[51] Y. Tan and B. Wei, "Observed behaviors of a long and deep excavation constructed by cut-and-cover technique in Shanghai soft clay," *Journal of Geotechnical and Geoenvironmental Engineering*, vol. 138, no. 1, pp. 69–88, 2012.

[52] Y.-J. Du, N.-J. Jiang, S.-Y. Liu, F. Jin, D. N. Singh, and A. J. Puppala, "Engineering properties and microstructural characteristics of cement-stabilized zinc-contaminated kaolin," *Canadian Geotechnical Journal*, vol. 51, no. 4, pp. 289–302, 2014.

[53] S.-L. Shen, J.-P. Wang, H.-N. Wu, Y.-S. Xu, G.-L. Ye, and Z.-Y. Yin, "Evaluation of hydraulic conductivity for both marine and deltaic deposits based on piezocone testing," *Ocean Engineering*, vol. 110, pp. 174–182, 2015.

[54] Z.-Y. Yin, Y.-F. Jin, H.-W. Huang, and S.-L. Shen, "Evolutionary polynomial regression based modelling of clay compressibility using an enhanced hybrid real-coded genetic algorithm," *Engineering Geology*, vol. 210, pp. 158–167, 2016.

[55] Z.-Y. Yin, P.-Y. Hicher, C. Dano, and Y.-F. Jin, "Modeling mechanical behavior of very coarse granular materials," *Journal of Engineering Mechanics*, vol. 143, no. 1, Article ID C4016006, 2017.

[56] Z.-Y. Yin, Y.-F. Jin, S.-L. Shen, and H.-W. Huang, "An efficient optimization method for identifying parameters of soft structured clay by an enhanced genetic algorithm and elastic–viscoplastic model," *Acta Geotechnica*, vol. 12, no. 4, pp. 849–867, 2017.

[57] Y. Tan and M. Li, "Measured performance of a 26 m deep top-down excavation in downtown Shanghai," *Canadian Geotechnical Journal*, vol. 48, no. 5, pp. 704–719, 2011.